International Journal of Disaster Risk Reduction 97 (2023) 104061

Contents lists available at ScienceDirect

International Journal of Disaster Risk Reduction

journal homepage: www.elsevier.com/locate/ijdrr

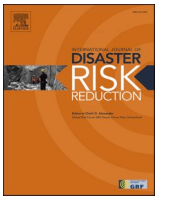

Application of landslide susceptibility towards urbanization suitability zonation in mountainous settings

Bipin Peethambaran [a,*], Ben Leshchinsky [b]

[a] Department of Forest Engineering, Resources, and Management, Oregon State University, 251 Peavy Hall, Corvallis, 97331, OR, USA
[b] Department of Forest Engineering, Resources and Management, Oregon State University, 236 Peavy Hall, Corvallis, 97331, OR, USA

ARTICLE INFO

Keywords:
Urban planning
Land suitability for urbanization
Urbanization suitability zonation
Landslide susceptibility map
Artificial intelligence
Geographic information systems

ABSTRACT

Amplified susceptibility to landslides poses challenges to sustainable and equitable urban development. Thus, in this study, we introduce an artificial intelligence and geographic information system-based approach, urbanization suitability zonation (USZ), for spatial assessment of land suitability for urbanization, which accounts multiple factors, including a focus on landslide susceptibility. Further, the proposed USZ is tailored to assess health of current urbanization patterns, depicting the driving factors behind it by establishing a best-case urbanization suitability (BUS) and weighted urbanization suitability (WUS). The BUS portrays a hypothetically ideal land suitability scenario as a function of equally weighted factors, while the WUS portrays land suitability changes when factors are weighted hierarchically. An examination of current development against the BUS provides idealness of current urbanization patterns. The WUS aids in assessing the significance of factors in influencing the current urbanization pattern, and checks its resemblance with the BUS. The mountainous Indian township of Mussoorie is selected as the study area to exercise the USZ by considering seven factors with different weights, and subsequently generated a BUS map and 7 WUS maps (WUS–I to VII), which all display urbanization suitability distribution in five different classes. The BUS map shows that ~98 % of current development falls in higher-suitability areas, indicating its preferability. Among the different WUS maps, the WUS-II aligns best with the BUS and current built-up, with slope gradient and transportation connectivity as key factors, and according to it, high-suitability areas are generally the central and south-facing slopes, while north-facing slopes are unsuitable, in general.

1. Introduction

Landslides are defined as the downward movement of soil and rock under the force of gravity, and are often triggered from rainfall, earthquakes, and/or anthropogenic activities (Varnes 1978). According to the World Health Organization, landslides account for over 10 % of all natural disasters worldwide and are responsible for over 4000 deaths annually, approximately. Controlled by a changing climate and increased landslide consequences, landslide disaster risk reduction has become an integral part of sustainable development, and it mostly addressed with help of landslide inventorying [1], susceptibility zonation [2,3], risk assessment [4,5], slope stability and runout assessment [6–8], monitoring [9,10] and slope stabilization measures [11], in general. Among them, landslide susceptibility zonation has seen major recent advances, attributed to availability of better geospatial data and remotely sensed observations. It is often broadly categorized as qualitative [12–14], and quantitative approaches [15,16]. Despite being widely

* Corresponding author.
E-mail address: bipin.peethambaran@oregonstate.edu (B. Peethambaran).

https://doi.org/10.1016/j.ijdrr.2023.104061
Received 11 July 2023; Received in revised form 11 October 2023; Accepted 12 October 2023
Available online 17 October 2023

researched, its direct applications, beyond as a standalone susceptibility map, are as an added variable for landslide risk and multi hazard mapping efforts [17–20].

Leveraging landslide susceptibility maps beyond their traditional confines for socially relevant applications such as urbanization is imperative in advancing disaster risk reduction and sustainable development. Urbanization, the modern-day manifestation of development, refers to the shift in population from rural areas to cities [21], which apparently impose development densification and challenges the development-sustainability balance. Land suitability for urbanization is one of decisive elements in urban planning, particularly in the era of climate changes and consequent natural hazards, along with other facets such as urban growth modelling [22], geo-environmental problems [23], urban groundwater [24], urban surface temperature [25], urban industry [26], etc. The land suitability models are generally overlay approaches [27,28], multi criteria statistical models [29–34], and opaque artificial intelligence models [35–38] based on various geo-environmental and socio-economic factors. The overlay approaches face drawbacks such as unsuitable map standardization and unverified assumptions about suitability criteria [39], while the rest account independence and uncertainty of factors, they heavily rely on input samples, which are presumed to be precise, accurate and unbiased [40]. Most notably, irrespective of the modelling approach, exposure to natural hazards was not given the deserving priority in general, with exceptions being [41] accounting flood inventory while [42] decided suitability solely based on multi-hazard exposure.

Therefore, the current research proposes an approach called urbanization suitability zonation (USZ), which primarily focuses on incorporation of spatial hazard probability, in this context, a landslide susceptibility map, along with other factors for generic assessments of land suitability for urbanization. Further, to overcome some of the shortcomings of earlier modelling approaches such as rigid classification, subjectivity, opacity and diversity adaptation, the USZ adopts Mamdani fuzzy logic/Mamdani-FIS [43] as the synthesizer. The Mamdani-FIS offers a system that embraces uncertainty, offers interpretability and flexibility with human-readable rules. Its ability to handle degrees of truth, rather than binary decisions, makes it especially apt for complex assessments where nuances are essential. Availability of such portable approaches may be helpful for planning authorities or even for individuals to make use of spatial hazard probability information for better-informed sustainable development through planning, forecasting and monitoring. The Mussoorie township is selected as a study example owing to its rapid development as an attraction in the Indian State of Uttarakhand, and its topographic constraints of surrounding mountainous terrain. Through this case study, the USZ's real-world application is demonstrated and discussed.

2. Methodology

2.1. Urbanization suitability zonation

Land-use suitability refers to the capacity of the land for the designated purposes [44], and governed by interaction of factors of physical, socio-economic, geo-environmental, ecological domains etc. Given the multi-criteria nature of land suitability, the USZ is designed to incorporate geo-environmental and socio-economic factors, in addition to landslide susceptibility whether they are of categorical or numerical nature. Beyond land suitability assessment for urbanization, use of the USZ enables inspection of the favourability of current development patterns and urban growth predictions, while relevance of various weighting factors can be explored through incorporation of the factor's sensitivity analysis.

In this context, the USZ model employs two specific sensitivity analysis concepts: BUS and WUS. The BUS is a hypothetical situation where all factors are equally relevant/weighted, whereas the WUS portrays land suitability corresponding to varying relevance/weights of factors. The applicability of BUS and WUS are pointed below.

- The hypothetically ideal BUS acts as the reference scale to assess the favourability of current urbanization/development pattern by inspecting the density of development in each suitability classes.
- The WUS helps in estimating relevance of factors in driving the urbanization in the area by accounting congruency of suitability classes and current development.
- Comparison of WUS with BUS in terms of similarity may express how ideal the considered WUS is.
- Based on the above three assessment and comparison, the best WUS shall be designated as the USZ map of the area. Interpretating the spatial distribution of its suitability classes may provide insights into possible urban growth trajectories.

The execution of USZ is straightforward cartographic modelling involving, 1) characterization of relevant factors, 2) simulation with Mamdani-FIS to generate the BUS and different WUS, and finally 3) assessment and comparison of BUS and WUSs.

2.1.1. Characterization of relevant factors

As stated earlier, land suitability assessment is a multi-criteria decision analysis, and broadly they fall into two categories, 'opportunities' and 'constraints' [40]. It must be taken into account that there exist no global guidelines that dictates the selection of these factors. Instead, the choice is effectively based on the attributes of the area of interest. Further, the categorization of factors, and their relevance or suitability estimation also hinges on local cultural preferences, regulations and practical constraints. For the application of Mamdani-FIS for USZ, it is essential to have the factors categorized, and relevance of each category of factors is estimated and expressed in human-readable form. The fundamentals of Mamdani-FIS are explained below.

2.1.2. Mamdani-FIS

The Mamdani-FIS a is widely applied fuzzy expert system model for modelling of system with ambiguities. It uses implicitly formulated linguistic rules instead of unambiguously defined algorithms to regulate the fuzzy inference mechanism. It has two fundamental segments, fuzzy inference system structure (fuzzifier and defuzzifier) and rule base (fuzzy if-then rules) required for the

inference mechanism. Fuzzifier transforms the crisp input to a fuzzy input with a degree of membership (between 0 and 1) to a set by using a membership function. The rule base links input variables (antecedents) to output variable (consequent), and the inference mechanism creates an optimum rational link between them by applying fuzzy operators. Whereas the defuzzifier transforms the conglomerated output membership function to a precise value [43].

Consider a general *i*th rule having multiple premises and antecedent of Mamdani fuzzy rule:

$$\text{Rule Ri}: f\ (x_1\ is\ A_{i1}) \bigotimes (x_2\ is\ A_{i2}) \bigotimes \ldots \bigotimes (x_n\ is\ A_{in})\ THEN (y\ is\ B_i)$$

$$\text{where}, i = 1, 2, \ldots, L \tag{1}$$

where $x = [x_1, x_2, \ldots, x_n]^T$ and y are crisp inputs and outputs with n-dimensional input variable and 1-dimensional output variable. A_{ij} $(j = 1, 2 \ldots, n)$ are linguistic variables corresponding to inputs and B_i are the fuzzy variable corresponding to outputs. The symbol $\bigotimes$ indicates the fuzzy OR or AND operation.

Fuzzification takes the crisp inputs and determine the degree to which they belong to each of the appropriate fuzzy sets via membership functions such as Triangular, Trapezoidal, Gaussian and Bell. The selection of appropriate membership function is largely dependent on nature of the problem and characteristics of data. For the current geo-spatial exercise, shape compatibility is considered for selecting the membership function combinations. Hence, two choices of combinations are possible, Gaussian and Bell or Triangular and Trapezoidal. However, previous study [45] indicate that the outcomes between these combinations might be minimal. Therefore, the current study uses the Triangular and Trapezoidal membership functions to construct the fuzzy inference system structure, which are mutually compatible, simple and easy to construct [46,47].

A Triangular membership function is specified by three parameters *a, b* and *c* which represent x-coordinates of three vertices of $\mu_{A_{ij}}$

$$\mu_{A_{ij}}(x_j) = \begin{cases} 0 & if\ \ x_j \le a \\ \dfrac{x_j - a}{b - a} & if\ a \le x_j \le b \\ \dfrac{c - x_j}{c - b} & if\ b \le x_j \le c \\ 0 & if\ x_j \ge c \end{cases} \tag{2}$$

A Trapezoidal membership function is specified by three parameters *a, b*, and *c* which represent x-coordinates of four vertices of $\mu_{A_{ij}}$

$$\mu_{A_{ij}}(x_j) = \begin{cases} 0 & if\ \ x_j < a\ or\ x_j > d \\ \dfrac{x_j - a}{b - a} & if\ a \le x_j \le b \\ 1 & if\ b \le x_j \le c \\ \dfrac{d - x_j}{d - c} & if\ c \le x_j \le d \end{cases} \tag{3}$$

The Inference mechanism establishes a logical connection between the input and output fuzzy sets using rules. Initially, a fuzzy number is obtained from a fuzzified input variable using OR/AND operation. To evaluate the disjunction of the rule antecedents, the OR fuzzy operation is used, which is expressed in the form of classical fuzzy operation union:

$$\mu_{Ai} = MAX\left\{\mu_{A_{i1}}(x_1), \mu_{A_{i2}}(x_2), \ldots, \mu_{A_{in}}(x_n)\right\} \tag{4}$$

Similarly, to evaluate the conjunction of the rule antecedents, the AND fuzzy operation intersection is used, and it is expressed as:

$$\mu_{A_i} = MIN\ \left\{\mu_{A_{i1}}(x_1), \mu_{A_{i2}}(x_2), \ldots, \mu_{A_{in}}(x_n)\right\} \tag{5}$$

The premise evaluation result is applied to the membership function of the consequent. The consequent part is reshaped with respect to the premise operation using fuzzy implications. Commonly min-max implication is used to perform the operation [48], which is defined in equations (6) and (7) respectively.

$$\mu_{Bi}(y) = \max_x min(\mu_{Ai}(x), \mu_{Ri}(x, y)) \tag{6}$$

$$\mu_{Bi}(y) = \max_x((1 - \mu_{Ai}(x))max(\mu_{Ai}(x) min\ \mu_{Ri}(x, y))) \tag{7}$$

Then aggregation of all consequent part of the fuzzy rule is performed by

$$\mu_B(y) = \max_{i=1,2,\ldots,L}(\mu_{Bi}(y)) \tag{8}$$

The aggregated fuzzy output is varied from 0 to 1 with respect to output variable and must be defuzzified to get the final crisp output. The centroid method is a commonly used strategy for defuzzification [48].

The defuzzified crisp output is represented as:

$$y^* = \frac{\int y\mu_B(y)dy}{\int \mu_B(y)dy} \tag{9}$$

2.1.3. Assessment and comparison of BUS and WUS

For the favourability inspection of current urbanization patterns, development proportions in opposition to BUS's suitability classes can be evaluated. This method may indicate how urban development aligns with hypothetically ideal suitability levels. Similarly, the development proportions shall be placed against the WUS's suitability classes to discern the influence of factors in prevailing urbanization pattern. To have the class specific comparison of WUS with BUS, a confusion matrix table can be used, in which the BUS can be considered as the truth, while the WUS serves as the prediction. Further, the overall similarity between the BUS and WUS shall be calculated the using following expression;

$$\mathrm{OS} = \sum(\mathrm{SP}) \Big/ \mathrm{sum}\ (\mathrm{SP} + \mathrm{DP}) \tag{10}$$

where, OS: overall similarity, SP: similar pixels in WUS, DP: dissimilar pixels in WUS.

3. Case study - urbanization suitability assessment of Mussoorie Township

A famous destination for tourism in the landslide prone Himalayan region, the Mussoorie township has been expanding rapidly to meet the economic and tourism demands for development; consequently, it serves as an interesting test location to explore urbanization patterns in context of landslide susceptibility. Throughout its history, slope instability [45] has been a major hazard that hindered sustainable development and environmental protections in the area. Despite many slope stability problems, construction practices in the township have been loosely regulated to accommodate the ever-rising influx of visitors. Most of the recent development is focused in the central ridge zone of the township (Fig. 3a), and generally consists of housing, hotels, shopping complexes, schools,

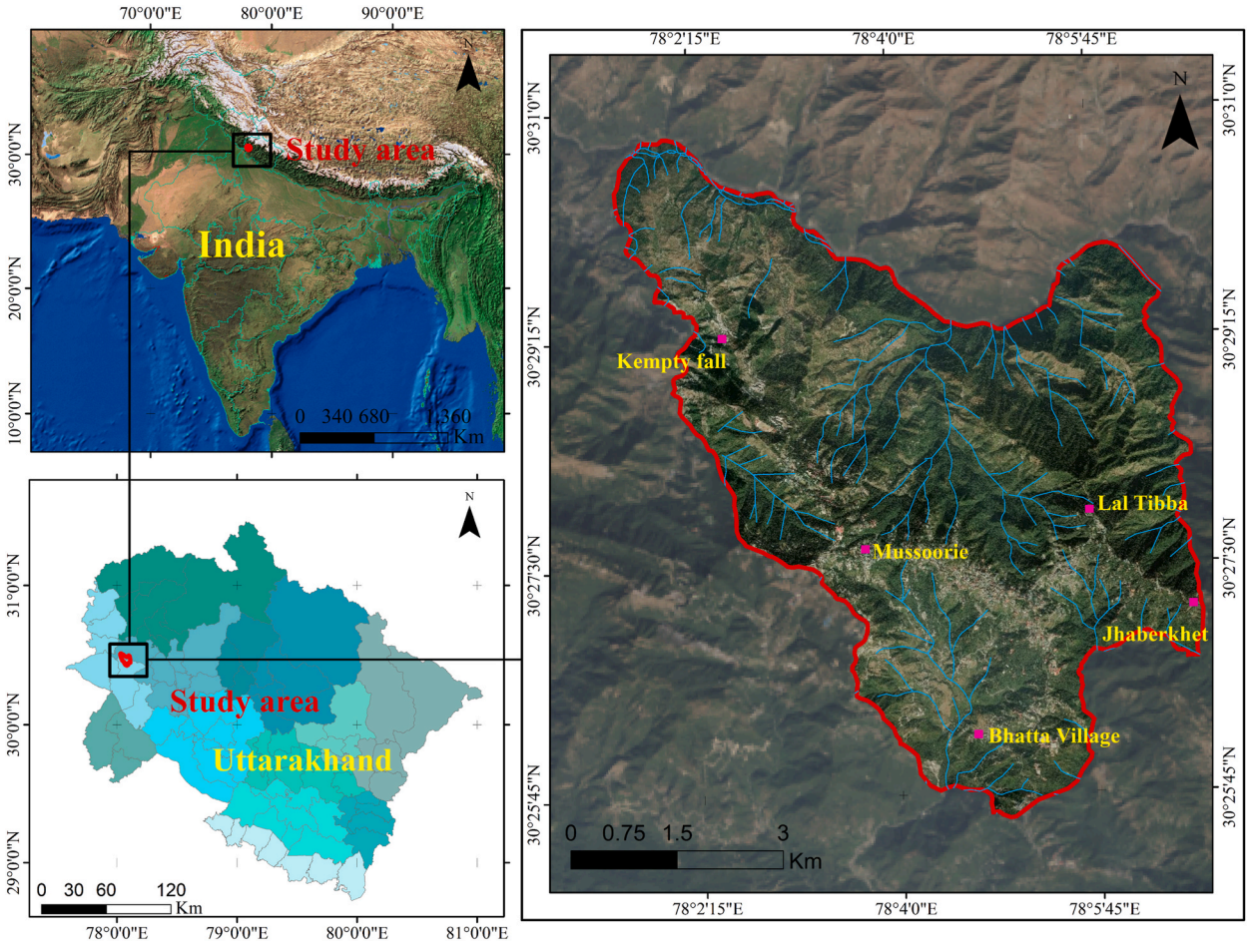

Fig. 1. Location map of study area.

and hospitals. Given the rate of expansion, an area of 43 km^2 in and around Mussoorie Township will be the focus of the study area (Fig. 1). The USZ of Mussoorie Township may primarily involves five steps (Fig. 2), which are: characterization of required factors, classification of factors and relevance estimation of categories of them, construction of Mamdani-FIS (FIS structure and rule base) and simulation of BUS and different WUS approaches, and assessment and comparison of BUS and WUS.

3.1. Characterization of factors for Mussoorie Township

Contemplating Mussoorie's history, challenges and developmental needs, a total of seven demonstrative factors focusing on geo-environmental, socio-economic and landslide susceptibility have been chosen for the evaluation. The significance of each factor in the present context, and their characterization is described herein. However, for any given site, the factors and hazard(s) of interest are up to the planners of the analysis.

3.1.1. Near-surface geologic material

Near-surface geologic material describes the basic geo-materials exposed in the area, and it often dictates safe and effective design and construction practices. It determines the stability of the structure and the cost of construction activities as well. Barren rock exposures are the least suitable for development as foundation excavation on barren rock is expensive or potentially infeasible. Further, maintaining transportation connectivity is also difficult in steep and rocky terrain. Conversely, maintaining and constructing linear infrastructure is often a feasible and cost-effective on more gentle slopes with fair soil thickness. Stratigraphically, study area is comprised of two Formations - Krol and Tal Formations of Mussoorie Group [49]. The near-surface geologic material map of the study area was prepared through fieldwork, by considering two broad categories of geo-materials: in-situ rocks and debris materials. Limestones or dolomitic limestones of Krol Formation exposed in the central part of study area, while quartzite of Tal Formation is present in the eastern part. On the other hand, the debris has been considered as two categories, shallow overburden (<5 m) and thick overburden (>5 m). A thematic map of slope constituting material is shown in Fig. 3b, and its classification is given in Table 1.

3.1.2. Slope gradient

Slope gradient is an important factor that governs construction practices, slope stability and infrastructure maintenance costs. In construction, gentle gradient slopes are generally more suitable compared to steeper slopes. A slope gradient map was prepared from a 15 m digital elevation model (DEM) (ALOS PALSAR) for the study area. The slope gradient ranges from 0 to 72.5° (Fig. 3c), which has been classified into five different classes based on the natural break classifier [50] for the evaluation (Table 1).

3.1.3. Transportation connectivity

Transportation connectivity or accessibility is an important socio-economic factor that determines the suitability of locations for

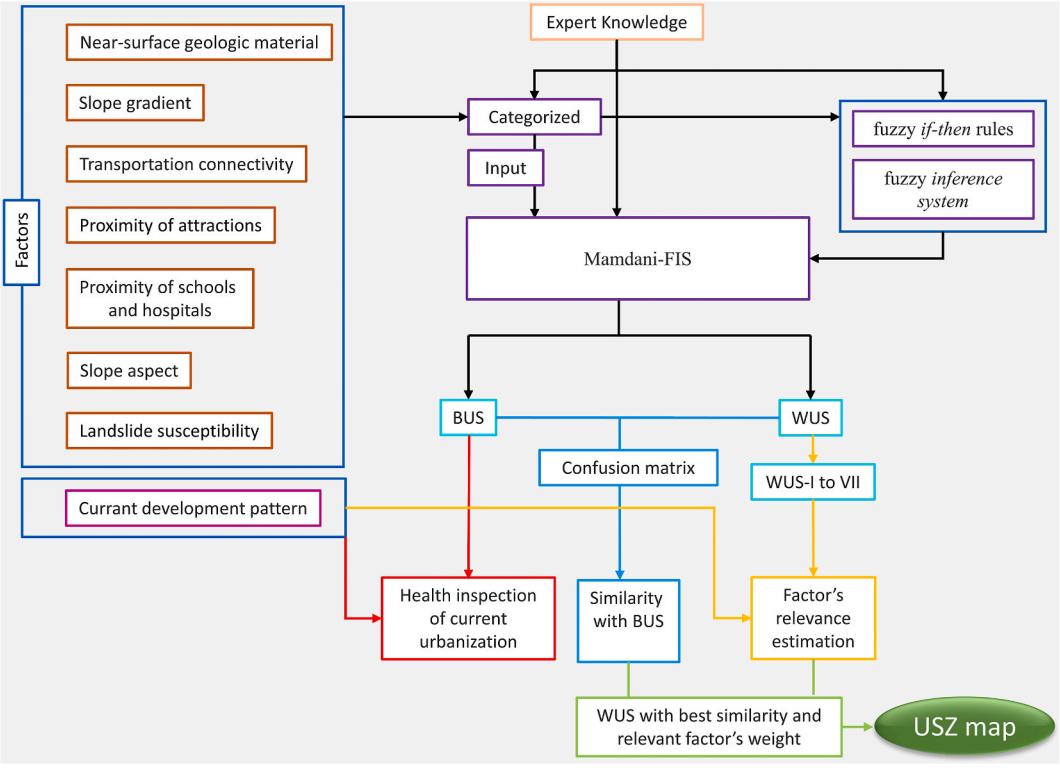

Fig. 2. Flowchart showing steps involved in urbanization suitability zonation of Mussoorie.

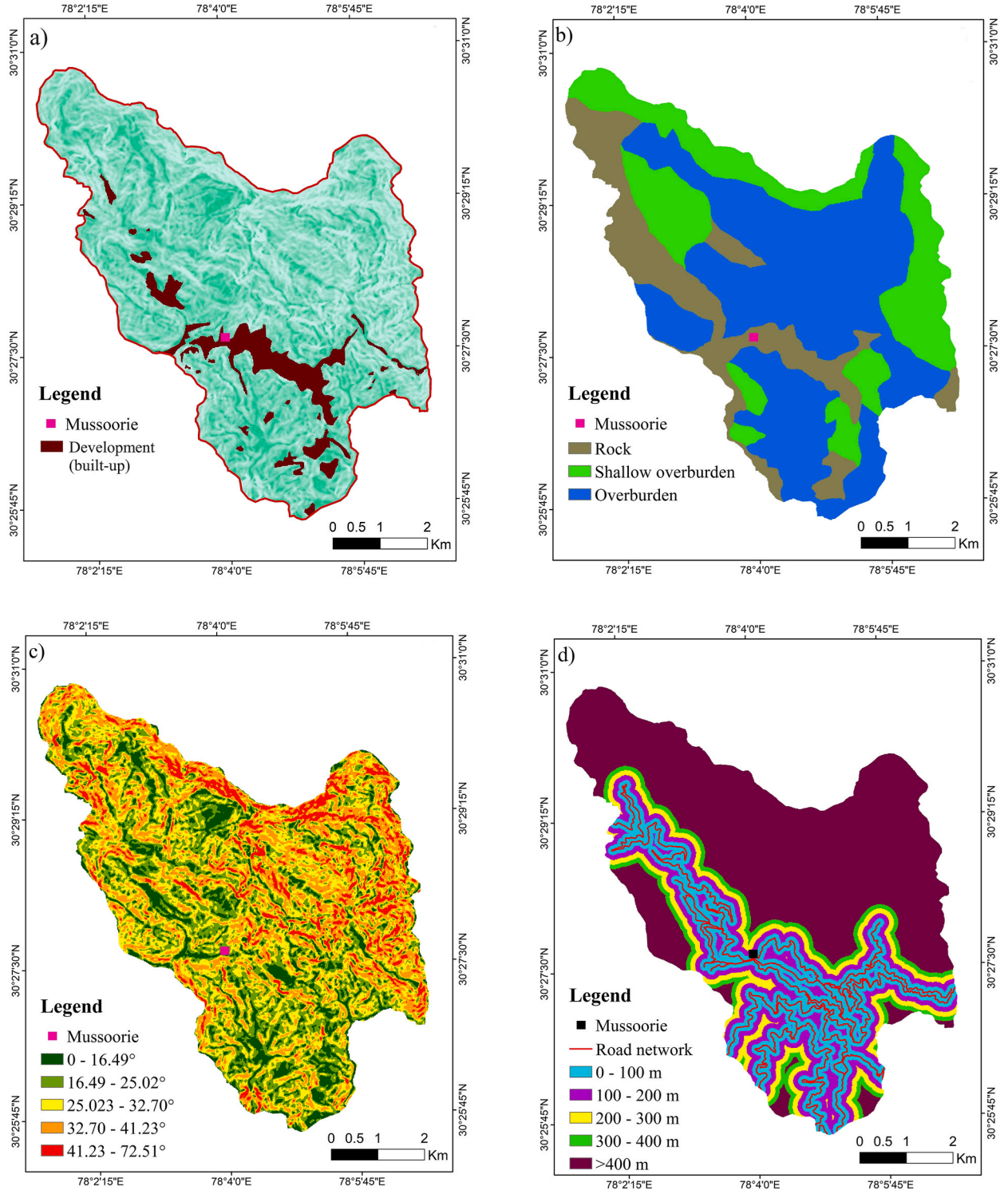

Fig. 3. Thematic maps of factors: a) Present development in Mussoorie Township, b) Near-surface geologic material, c) slope gradient, d) transportation connectivity, e) proximity of attractions, f) proximity of schools and hospitals, g) slope aspect, h) landslide susceptibility.

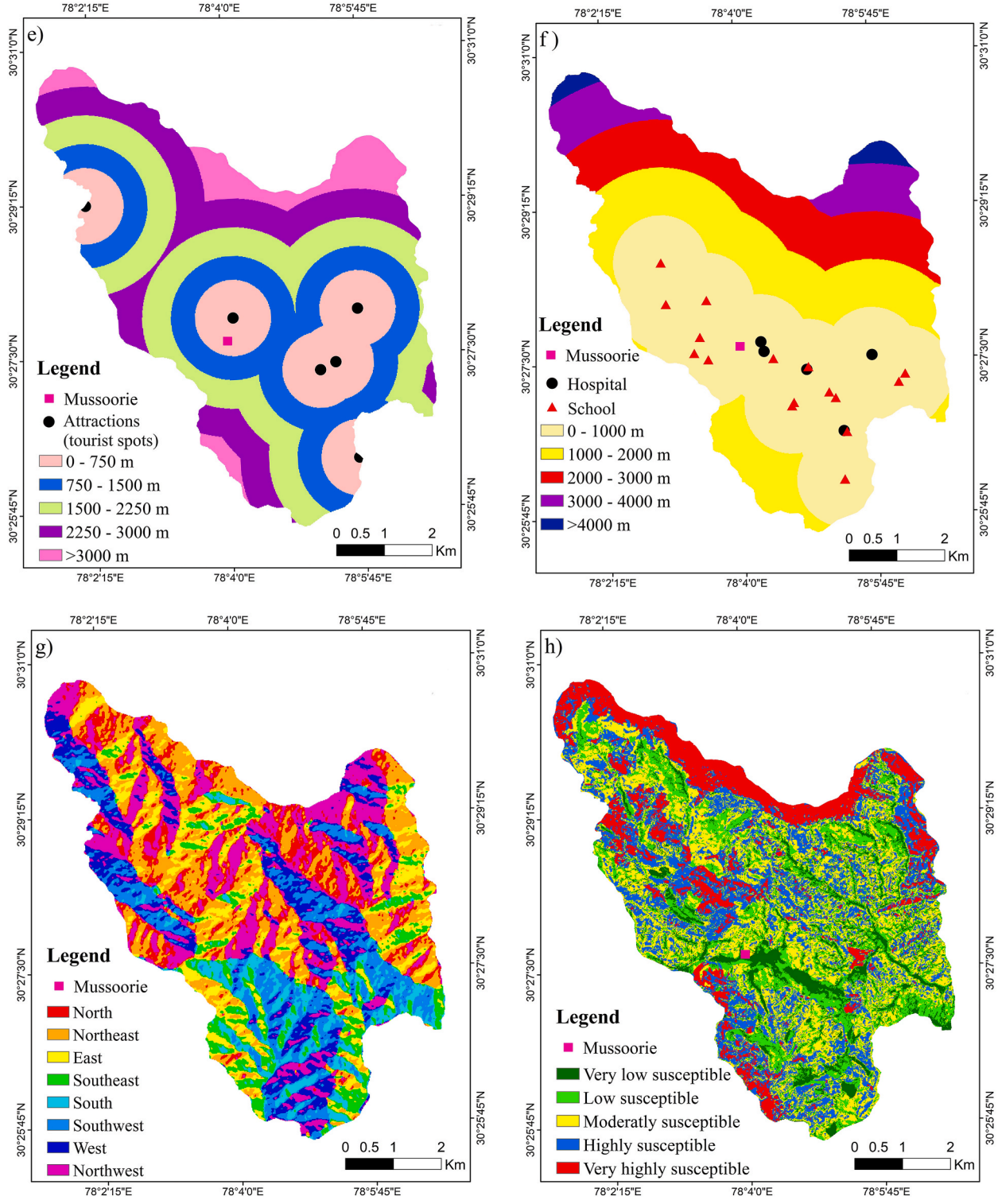

Fig. 3. (*continued*).

Table 1
Classification of factors and mean value of categories.

Factor	Categories	Mean of categories
Near-surface geologic material	Rock	–
	Shallow overburden	–
	Overburden	–
Slope gradient	Very gentle (0–16.49°)	8.25°
	Gentle (16.49–25.02°)	20.76°
	Moderate (25.02–32.70°)	28.86°
	Steep (32.70–41.23°)	36.97°
	Very steep (41.23–72.51°)	56.87°
Transportation connectivity	Buffer zone I (0–100 m)	50 m
	Buffer zone II (100–200 m)	150 m
	Buffer zone III (200–300 m)	250 m
	Buffer zone IV (300–400 m)	350 m
	Buffer zone V (400–2610 m)	1505 m
Proximity of attractions	Very near (0–750 m)	375
	Near (750–1500 m)	1125
	Moderate (1500-1250 m)	1875
	Far (1250–3000 m)	2625
	Very far (>3000 m)	3350
Proximity of schools and hospitals	Very close (0–1000 m)	500 m
	Close (1000–2000 m)	1500 m
	Moderate (2000–3000 m)	2500 m
	Far (3000–4000 m)	3500 m
	Very far (>4000 m)	4250 m
Slope aspect	Flat (−1)	−1
	North (0–22.5°) and (337.5–360°)	11.2° & 348.7°
	Northeast (22.5–67.5°)	45°
	East (67.5–112.5°)	90°
	Southeast (112.5–157.5°)	135°
	South (157.5–202.5°)	180°
	Southwest (202.5–247.5°)	225°
	West (247.5–292.5°)	270°
	Northwest (292.5–337.5°)	315°
Landslide susceptibility	Very low (−3.459388971 - 0.091714957)	−1.683837007
	Low (0.091714957–0.335853352)	0.213784155
	Moderate (0.335853352–0.557797348)	0.44682535
	High (0.557797348–0.801935743)	0.679866546
	Very high (0.801935743–2.200182915)	1.501059329

urbanization and economy. An existing network of roads facilitates construction, and provides access to nearby well-established townships to enhance its commercial growth through trade, tourism, etc. The road network of Mussoorie Township was prepared using Google Earth layers [51] (Fig. 3d). To incorporate the road network in the analysis, five buffer zones at an interval of 100 m were considered (Table 1).

3.1.4. Proximity of attractions

The Mussoorie region is one of the most famous Himalayan tourist destinations, and the tourism industry contributes greatly to its economy. Urbanization close to cultural attractions not only enhances its economic growth, but also fosters social developments. Consequently, owing to frequent development around these cultural centres, we include their location as a factor in this analysis. The list of major tourist locations in the study area are collected from the Mussoorie Urban Local Body (https://www.nppmussoorie.com/index.php), and a thematic map was prepared with the aid of Google Earth [51], which shows the tourist centres a as points (Fig. 3e). For the analysis, five classes, namely, very near, near, moderate, far and very far were considered at 750 m interval around the spots (Table 1).

3.1.5. Proximity of schools and hospitals

Schools and health services are fundamental building blocks of civilization and consequently development. A region facilitated with ample and easily accessible educational and health infrastructure is often regarded as suitable for habitation, as it ensures liveability and socio-economic growth. The list of schools and hospitals in the study area are obtained from the Mussoorie Urban Local Body (https://www.nppmussoorie.com/index.php), and their geographical locations are marked with aid of Google Earth [51] as points to prepare the thematic map (Fig. 3f). For the evaluation, five classes, namely, very close, close, moderate, far and very far were considered at 1000 m interval around them (Table 1).

3.1.6. Slope aspect

The slope aspect is an environmental factor that is often a secondary parameter in urban planning; however, it is a significant factor influencing sunlight exposure, vegetation, microclimate variations, and more. Exposure to sunlight has a significant role on slope stability, as it helps slopes dry quickly and enhances growth of vegetation and their stabilizing roots. Beyond its environmental

relevance, exposure to sunlight is desirable for community well-being and health. In this regard, the east and west facing slopes, which receives more sunlight in the morning and evening are most suitable than other slopes. Further, micro-climate variations may also play a vital role in the sustainable and smart development of an area, particularly in mountainous terrain. In Mussoorie, the north facing slopes experience more snowfall and colder temperatures than the south facing slopes, causing microclimate variations in the township. A slope aspect map of study area was prepared from the DEM (Fig. 3g) at 15 m resolution, and its preferred classification is given in Table 1.

3.1.7. *Landslide susceptibility*

Landslide susceptibility expresses the propensity to slope instability in an area, often graded on a scale, such as from very low to very high. The graded propensity serves as predictive tool, allowing for better-informed planning and disaster preparedness. In the context of urbanization or construction, the very low susceptible areas are highly suitable, whereas the very high susceptible areas are

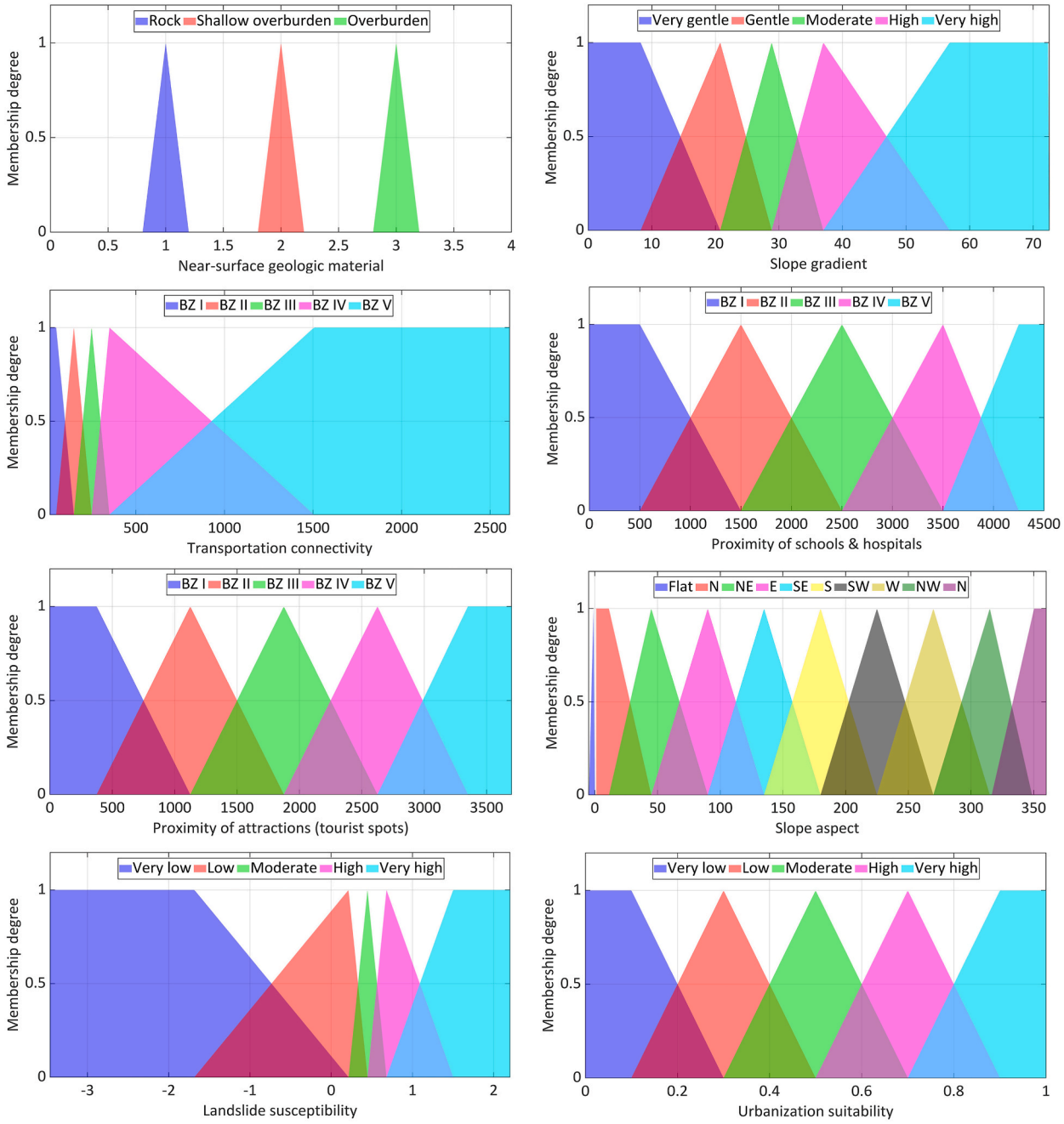

Fig. 4. Fuzzy inference system structure of the Mamdani-FIS model.

least suitable. This study uses the landslide susceptibility map of Mussoorie (Fig. 3h) prepared by [52] on meso-scale. This map was generated using a supervised machine learning model, extreme learning adaptive neuro-fuzzy (ELANFIS) [53–55], based on inherent causative factors such lithology, land use & land cover, slope gradient, slope aspect, lineament, elevation, curvature, and topographic wetness index. As per this map (Figs. 3h), 16.10 % area fall in the very high susceptibility class, and the proportions of the study area with high, moderate, low and very low susceptibilities are, 26.33, 27.72, 20.80 9.04 %, respectively [52]. The landslide susceptibility classes, and their corresponding susceptibility indexes according to the natural break classifier [50] are given in Table 1.

3.2. Mamdani-FIS model construction and simulation

As stated in methodology, the Mamdani fuzzy inference system has two segments, fuzzy inference system/membership function structure and rule base. The Triangular and Trapezoidal membership functions have been used to fabricate the fuzzifier and defuzzifier structure, according to the classification of factors given in Table 1. The total number of factors are seven, and the categories between them are 37, thus, the fuzzifier has 7 input membership functions and 37 individual membership functions representing each category of their respective factor. A maximum of 50 % interaction is considered between membership functions representing the categories of numerical factors to account optimum fuzziness between them, in which highest degree of membership is given to the mean value (Table 1) of each category [56]. While for the categorical factor, mutually non-interacting membership functions were chosen for representing the individual categories of a factor. Five classes of suitability are targeted viz. very low suitability (VLS), low suitability (LS), moderate suitability (MS), high suitability (HS) and very high suitability (VHS), thus, the defuzzifier consists of 5 individual representative membership functions at 50 % of overlap with each other [56]. The fuzzy rule base consists of 37 non-combination rules in conventional consequent-antecedent format, establishing the suitability of each category of factors for urbanization. The fuzzy inference system structure is shown in Fig. 4, and the rule base is given in Table 2.

The BUS and WUS were executed by assigning numerical weights to factors in Mamdani-FIS to incorporate the sensitivity analysis. The weight assigning system in Mamdani-FIS ranges from 0 to 1, where 0 indicates least/no relevance and 1 indicates highest/full relevance, relatively. For BUS, all factors are having a weight of 1, implying equal relevance, whereas for WUS, weights are randomly varied from 0.1 to 1 for all factors. The weights assigned to the factors in WUS are rotated in such a way that each factor, in turn, is assigned the highest and the lowest weights, which apparently implies the relevance. It must be noted that the weights establish only a

Table 2
Fuzzy if-then rules formulated based on expert knowledge.

Rule No.	Consequent	Antecedent
1	If near-surface geologic material is rock	Then urbanization suitability is low
2	If near-surface geologic material is shallow overburden	Then urbanization suitability is moderate
3	If near-surface geologic material is overburden	Then urbanization suitability is high
4	If slope gradient is very gentle	Then urbanization suitability is very high
5	If slope gradient is gentle	Then US is high
6	If slope gradient is moderate	Then urbanization suitability is moderate
7	If slope gradient is steep	Then urbanization suitability is low
8	If slope gradient is very steep	Then urbanization suitability is very low
9	If transportation connectivity buffer zone is I	Then urbanization suitability is very high
10	If transportation connectivity buffer zone is II	Then urbanization suitability is high
11	If transportation connectivity buffer zone is III	Then urbanization suitability is moderate
12	If transportation connectivity buffer zone is IV	Then urbanization suitability is low
13	If transportation connectivity buffer zone is V	Then urbanization suitability is very low
14	If proximity of attractions is very near	Then urbanization suitability is very high
15	If proximity of attractions is near	Then urbanization suitability is high
16	If proximity of attractions is moderate	Then urbanization suitability is moderate
17	If proximity of attractions is far	Then urbanization suitability is low
18	If proximity of attractions is very far	Then urbanization suitability is very low
19	If proximity of schools and hospitals is very close	Then urbanization suitability is very high
20	If proximity of schools and hospitals is close	Then urbanization suitability is high
21	If proximity of schools and hospitals is moderate	Then urbanization suitability is moderate
22	If proximity of schools and hospitals is far	Then urbanization suitability is low
23	If proximity of schools and hospitals is very far	Then urbanization suitability is very low
24	If slope aspect is flat	Then urbanization suitability is very low
25	If slope aspect is north	Then urbanization suitability is very low
26	If slope aspect is northeast	Then urbanization suitability is low
27	If slope aspect is east	Then urbanization suitability is very high
28	If slope aspect is southeast	Then urbanization suitability is high
29	If slope aspect is south	Then urbanization suitability is moderate
30	If slope aspect is southwest	Then urbanization suitability is moderate
31	If slope aspect is west	Then urbanization suitability is very high
32	If slope aspect is northwest	Then urbanization suitability is low
33	If landslide susceptibility is very low	Then urbanization suitability is very high
34	If landslide susceptibility is low	Then urbanization suitability is high
35	If landslide susceptibility is moderate	Then urbanization suitability is moderate
36	If landslide susceptibility is high	Then urbanization suitability is low
37	If landslide susceptibility is very high	Then urbanization suitability is very low

Table 3
Weights of factors for BUS and different WUS.

Factor	Weights							
	BUS	WUS-I	WUS-II	WUS-III	WUS-IV	WUS-V	WUS-VI	WUS-VII
Near-surface geologic material	1	1	0.1	0.25	0.4	0.55	0.7	0.85
Slope gradient	1	0.85	1	0.1	0.25	0.4	0.55	0.7
Transportation connectivity	1	0.7	0.85	1	0.1	0.25	0.4	0.55
Proximity of attractions	1	0.55	0.7	0.85	1	0.1	0.25	0.4
Proximity of schools and hospitals	1	0.4	0.55	0.7	0.85	1	0.1	0.25
Slope aspect	1	0.25	0.4	0.55	0.7	0.85	1	0.1
Landslide susceptibility	1	0.1	0.25	0.4	0.55	0.7	0.85	1

relative importance and are not highly sensitive to its numerical values. Hence, a BUS and sevenWUS scenarios are considered, and their corresponding weights are given in Table 3.

The simulated urbanization suitability indexes of BUS and WUSs are subsequently classified with Jenks natural break classifier [50] to create the BUS and seven WUS maps, namely WUS-I to VII (shown in Fig. 5), and the distribution of suitability classes in each map, corresponding development are given in Table 4. The results of confusion matrix analysis between the BUS and different WUS is shown in Fig. 6.

4. Results

The BUS (Fig. 5a) displays an error-free spatial distribution of suitability classes with no prominent trace of factors. On the BUS, the VHS class is distributed in the central part of the study area along the ridge zone. As the distance increases from the central area, suitability gradually reduces. However, the VLS class is predominantly distributed towards the northern end of the study area, whereas the southern side scores high on overall suitability, though sparse occurrence of LS is inferred. According to the distribution of suitability classes given in Table 4, VHS accounts 20.49 % of the area, and it hosts a total of 71.28 % of the present development, while 27.55 % of present development falls in the highly suitable area that account for 28.19 % of the study area. The MF class accounts a share of 26.01 % of the area, and hosts 1.17 % of current development, while VLS and LS classes devoid of development though they account a fair share of 7.09 and 18.22 % of the area, respectively.

The different WUS scenarios display an interesting and more or less similar spatial distribution pattern of classes. In WUS-I and II, the spatial distribution of classes is similar, with the south, southwest, and ridge zones falling into HS and VHS classes, however, patches of VLS class in the southern side is observed in the WUS-I. In terms of class per area percentage, both WUS-I and II are largely analogous, but the development concentrations differ significantly (Table 4). The development concentration per class shows an increasing trend on both WUS-I and II, in general, but notably, a sizeable segregation is observed for VLS and MS on the WUS-I, and it rises to 53.77 % for VHS class, whereas for WUS-II, fair hosting is observed from HS class and the VHS class hosts an impressive 75.77 % (Table 4).

The WUS-III (Fig. 5d) showcases a nested spatial distribution of classes that appears unrealistic. The VHS class is concentrated in the central area, while other suitability classes are spread out sequentially. However, the distribution statistics have similarities with WUS-II with as HS accounting the highest share of 27.89 %, which hosts 15.49 % of development, while the VHS class has 24.05 % of land share and accommodates 84.28 % of the development. Moving to WUS-IV (Fig. 5e), the spatial distribution and statistics are alike the previous scenarios, with the HS class accounting for the largest share of 30.07 %, while the VHS class has 21.88 % of area, which hosts 65.96 % of development (Table 4). On WUS-V (Fig. 5f), the LS class expands to cover 18.98 % of the land, while the MS and HS classes encompass 25.96 % and 27.72 % of the area, respectively. Surprisingly, the VHS class occupies only 19.80 % of the land, yet it hosts a substantial 57.78 % of the development areas. Transitioning to WUS-VI (Fig. 5g), the LS and VLS classes poses for 11.42 % and 21.07 % of the area, respectively, with relatively smaller percentage of development. The VHS class covers 16.23 % of the area but accommodates only 47.53 % of the development. Contrastingly, in WUS-VII (Fig. 5h), the VLS, LS and VHS classes' area share diminishes to 8.74 %, 20.21 % and 18.66 %, respectively, although the development per class show an increasing trend (Table 4).

The confusion matrix (Fig. 6) demonstrates the similarity of different WUS with the BUS, and it portrays the sensitivity of factors in deciding the suitability. The WUS-I has an overall similarity of 75.72 % with BUS (Fig. 6a) as the VLS and VHS classes have high similarity even though dissimilarity is observed for LS, MS and HS classes. The very same proportion of class similarity is observed for WUS-II with BUS, however; the overall similarity with BUS has increased to 77.09 % (Fig. 6b), attributed to increase in matching pixels for all the classes, except MS, compared to WUS-I. For the WUS-III, matching pixels experiences a fall in number compared to the earlier map, except for the VHS class. Apparently, its overall similarity with the BUS is settled to 70.89 % (Fig. 6c), and in the same vein, drop in matching pixel's number for VLS, LS, and VHS classes caused WUS-IV to have an overall similarity of 67.63 % (Fig. 6d) with the BUS. Conversely, the WUS-V's resemblance with the BUS rises to 73.21 % (Fig. 6e), though dissimilarity is observed for all the classes. Further, for WUS-VI and VII, the proportions of dissimilarity for all the classes have shown an increasing trend, and eventually curtailing the resemblance with BUS to 60.75 % (Figs. 6f) and 65.92 % (Fig. 6g), respectively.

5. Discussion

According to the BUS, the HS and VHS classes are distributed along the central ridge zone, and the south, south-west and south-east

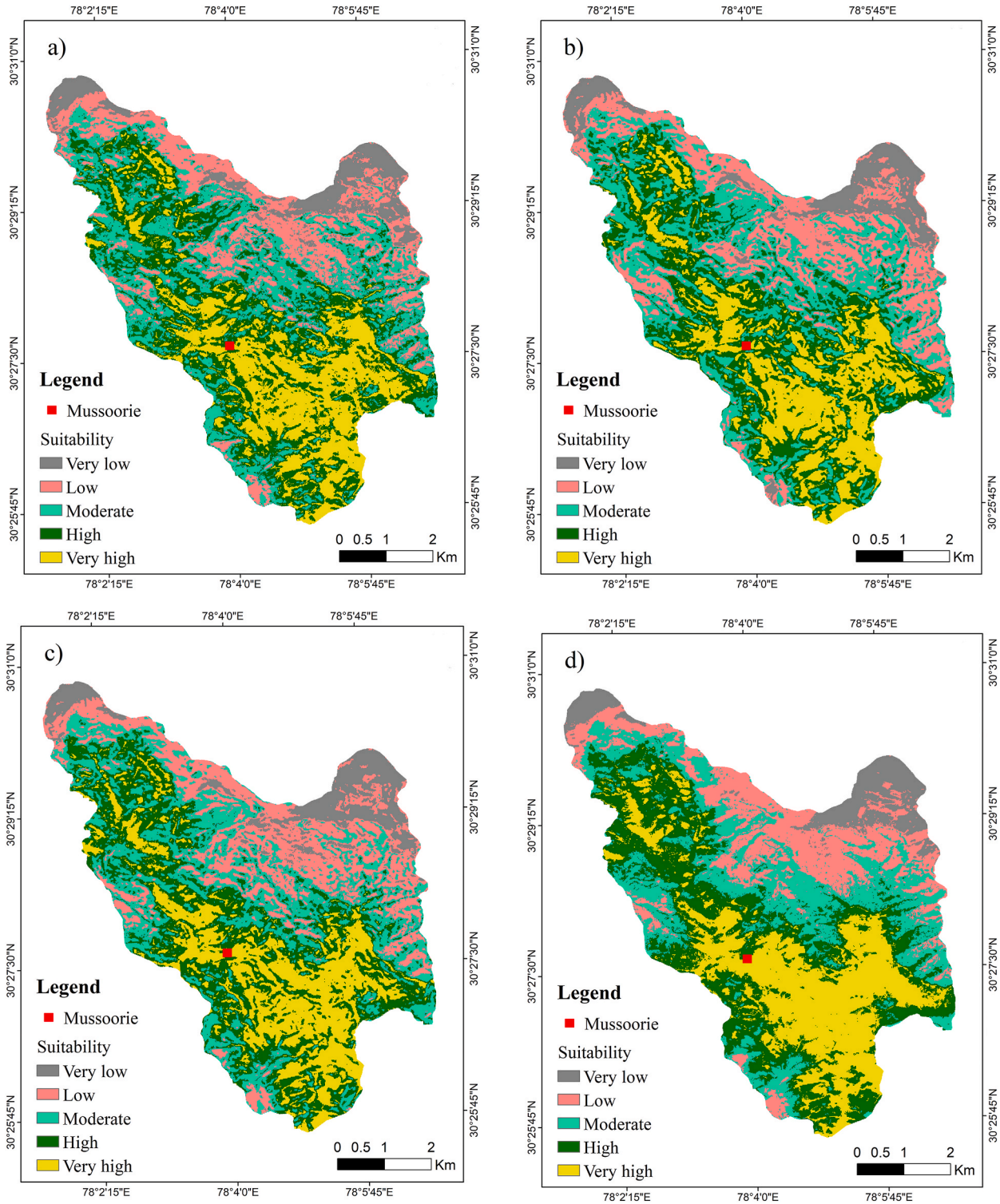

Fig. 5. BUS and WUS maps of Mussoorie.

facing areas. The higher suitability of these areas compared to the north-facing slopes might be attributed to preferable slope gradient, better transportation connectivity and lower landslide susceptibility. Further, the substantial proportions of current development within the HS and VHS classes of the BUS underscores the preferability of current urbanization pattern, given study areas' prospects.

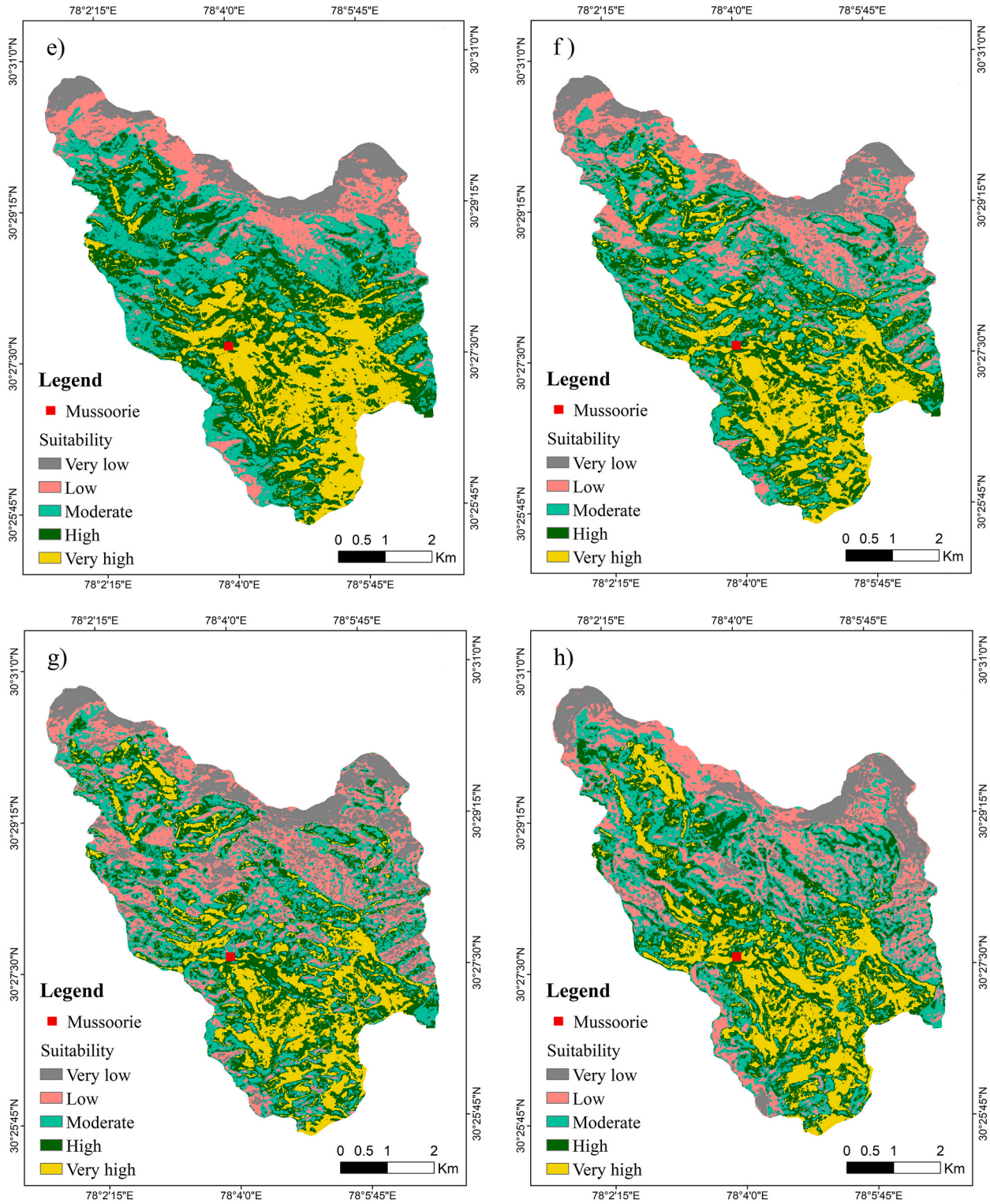

Fig. 5. (*continued*).

However, weighing all the factors equally might not be practical, particularly for a mountainous township, hence, this scenario has been portrayed with the WUS approach. Since it is an existing township and current development/urbanization is congruent with the BUS, spatial distribution quality, competency to host current development on VHS and HS classes and similarity with BUS have been

Table 4
Distribution of suitability classes in oppose to current development.

Suitability class	Percentage of class	Percentage of development (built-up)
BUS		
VLS	7.09	0
LS	18.22	0
MS	26.01	1.17
HS	28.19	27.55
VHS	20.49	71.28
WUS-I		
VLS	7.68	0.00
LS	20.19	0.06
MS	26.52	8.16
HS	26.24	38.02
VHS	19.38	53.77
WUS-II		
VLS	7.74	0.00
LS	20.24	0.00
MS	25.17	0.83
HS	27.11	23.40
VHS	19.73	75.77
WUS-III		
VLS	6.97	0.00
LS	17.95	0.00
MS	23.15	0.23
HS	27.88	15.49
VHS	24.05	84.28
WUS-IV		
VLS	7.55	0.00
LS	13.33	0.01
MS	27.17	3.25
HS	30.07	30.78
VHS	21.88	65.96
WUS-V		
VLS	8.36	0.00
LS	18.16	0.11
MS	25.96	5.83
HS	27.72	36.28
VHS	19.80	57.78
WUS-VI		
VLS	11.42	0.01
LS	21.07	0.85
MS	25.98	13.92
HS	25.30	37.69
VHS	16.23	47.53
WUS-VII		
VLS	8.74	0.00
LS	20.21	0.14
MS	26.49	3.78
HS	25.91	28.77
VHS	18.66	67.31

measured for all the WUS scenarios.

Giving top priority to lithology and slope gradient for WUS-I (Table 3), the competency to host developed areas on VHS is low, although it has reasonable similarity with the BUS, and spatial distribution quality. When slope gradient and transportation connectivity are of highest relevance for WUS-II, the VHS class hosts significantly high percentage of development in addition to achieving the highest similarity with the BUS, and acceptable spatial distribution quality. On the other hand, with slope gradient being moved farthest down the order and transportation connectivity is prioritized for making WUS-III, the spatial distribution quality is considerably degraded, although the development density within the VHS class and similarity with BUS is reasonable. Further, as the slope gradient's relevance is elevated and transportation connectivity has the least relevance for making WUS-IV, the spatial distribution quality has improved, but the development density on predicted VHS class and the overall similarity with BUS are compromised. Similarly, with relatively high relevance for proximity of schools and hospitals and slope aspect for WUS-V and VI, the development concentration on VHS class and similarity with BUS are low, though spatial distribution is reasonable. In case of WUS-VII, as the landslide susceptibility is prioritized, the spatial distribution quality was found to be reasonable, but the proportion of development on VHS and resemblance with BUS were found to be mediocre.

In this regard, the WUS-II was found to be in great agreement for all the measures considered, and was selected as the optimal urbanization suitability map of Mussoorie. Inferring the weightages considered for WUS-II, it may be possible to interpret that the current urbanization was driven primarily by slope gradient and transportation connectivity. Further, the sensitivity of factors

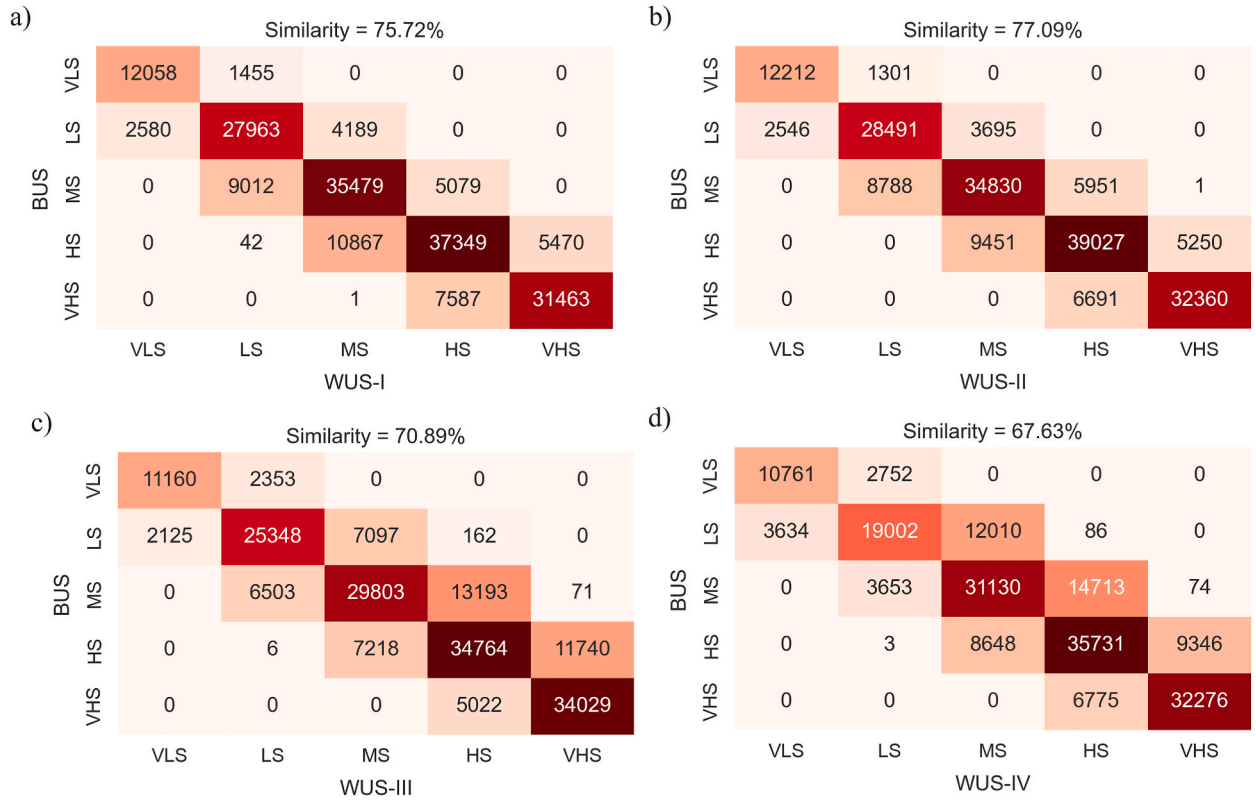

Fig. 6. Confusion matrix analysis between the BUS and WUS-I to VII, from panels a) to g), respectively.

portrayed with different WUS scenarios also indicate that the suitability is highly sensitive to the weightage of slope gradient and transportation connectivity than others. Based on the spatial distribution of suitability classes on WUS-II, the central area, along the ridge, is falling in the VHS class, and the nearby south facing slopes belong to the HS class. Further, looking at the WUS-II, it may be possible to predict that the urban growth may continue to take place along the ridge zone, however, the south-west, south and south-east facing slopes on the southern side may also experience higher degree of urbanization in the future as they also fall in the highly suitable classes.

6. Conclusions

The proportion of people living in urban environments is rising, imposing added demands for construction-driven urbanization. Landslides, one of the most widespread and frequently occurring natural hazards, present an unprecedented risk to urbanization, particularly in mountainous regions. Timely recognition of suitable areas in hazard prone regions will prevent undesired urban sprawl and promotes sustainable development. Hence, the current research attempts incorporation of slope stability in the form of landslide susceptibility map for generic land suitability assessment for urbanization by presenting the USZ approach. Land suitability for urbanization is influenced by various geo-environmental, socio-economic and natural hazard factors, and their complex interrelation and spatial variation makes it a challenging assignment. Therefore, the USZ uses the Mamdani-FIS to simulate urbanization suitability as a function of considered factors based on implicitly defined rules, attributed to its capability to curb subjectivity of expert choices, transparency, ability to account uncertainties and more saliently, its efficiency to express complex interests such as demographic or religious preferences in the form of natural language rules.

The USZ has been exercised for the Himalayan township of Mussoorie by considering seven factors, and relevance of them was decided based on expert knowledge. As per the BUS, the township's current development pattern aligns well with its limits and requirements. Based on the urbanization suitability map, WUS-II, around 19.73 % of the area is very highly suitable for urbanization, and transportation connectivity and slope gradients are identified as the most influencing factors behind its current urbanization pattern. Given the influence of these factors, 27.11 and 25.17 % of the area fall in the HS and MS classes, and they may or will be targeted for urban growth in the future without significant development of transportation connectivity.

The urbanization suitability map of Mussoorie, WUS-II, may be of help for urban planning of Mussoorie. Similar application of USZ for other areas may make utilization of high number of landslide susceptibility maps are being produced worldwide for equitable and sustainable development. Though this study used only the landslide susceptibility map, similar thematic maps corresponding to flood, wildfire, drought, earthquake, etc. or multi-hazard susceptibility can be incorporated for USZ in a similar manner. If it is attempted for

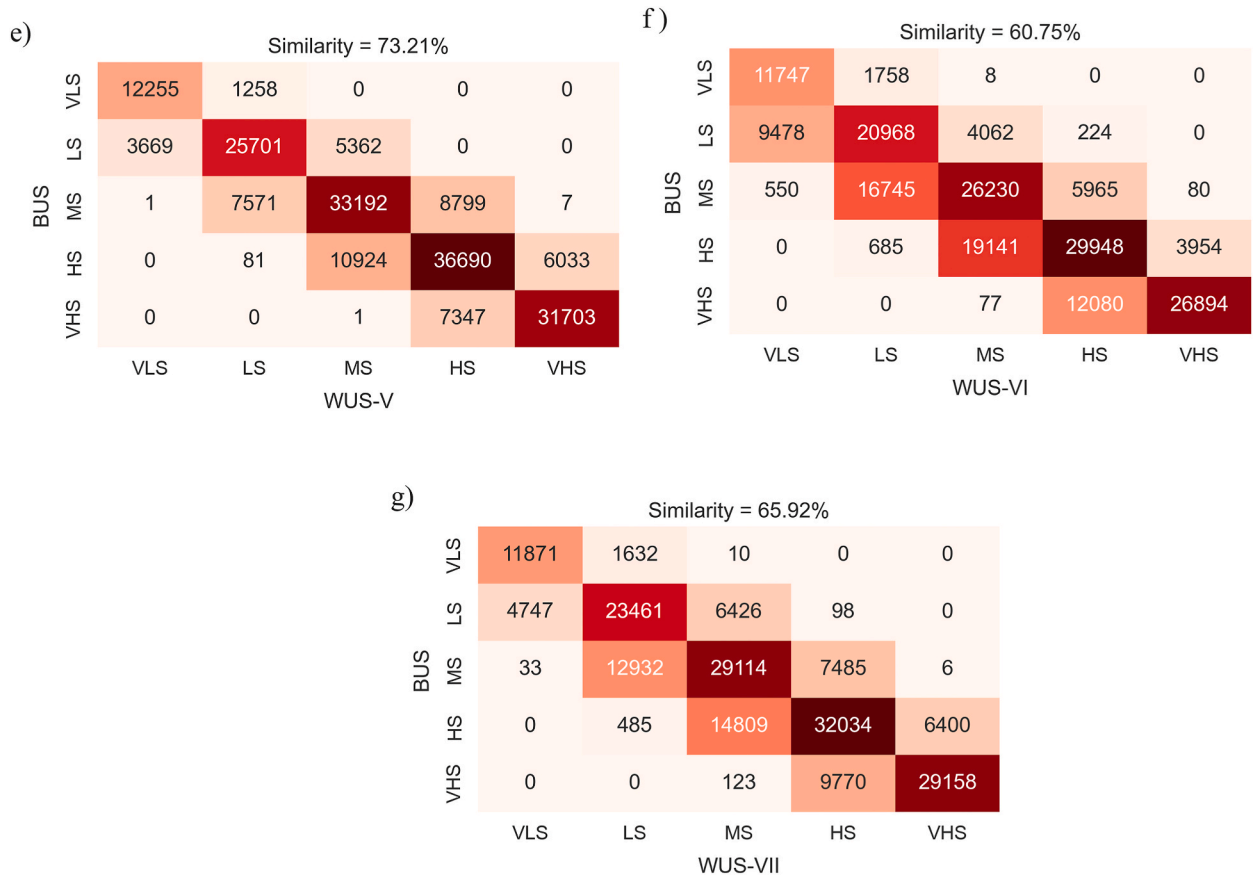

Fig. 6. (*continued*).

an existing township, exercise of BUS and WUS may be required, however; application to virgin areas may need only BUS, unless hierarchy of factors is preferred. Further, the present case study shall only be treated as a basic framework, and the number of factors, their classification, and associated rules shall be customized to specific user preferences and requirements.

Funding

The second author acknowledges support from the National Institute of Food and Agriculture (NIFA) under grant No. 2021-67022-35908, the US National Science Foundation under grant CMMI-2050047, and USDA Mcintire-Stennis project OREZ-FERM-898.

Declaration of competing interest

The authors declare that they have no known competing financial interests or personal relationships that could have appeared to influence the work reported in this paper.

Data availability

Data will be made available on request.

Acknowledgement

The authors would like to express their gratitude to the editors and to anonymous reviewers for their constructive and valuable feedback. It greatly helped improve this manuscript.

References

[1] P. Amatya, D. Kirschbaum, T. Stanley, H. Tanyas, Landslide mapping using object-based image analysis and open source tools, Eng. Geol. 282 (2021), 106000, https://doi.org/10.1016/j.enggeo.2021.106000.
[2] R. Anbalagan, Landslide hazard evaluation and zonation mapping in mountainous terrain, Eng. Geol. 32 (1992) 269–277, https://doi.org/10.1016/0013-7952(92)90053-2.

[3] G. Karakas, S. Kocaman, C. Gokceoglu, Comprehensive performance assessment of landslide susceptibility mapping with MLP and random forest: a case study after Elazig earthquake (24 Jan 2020, Mw 6.8), Turkey, Environ. Earth Sci. 81 (2022), https://doi.org/10.1007/s12665-022-10225-y.
[4] F. de L.R. Listo, B. Carvalho Vieira, Mapping of risk and susceptibility of shallow-landslide in the city of São Paulo, Brazil, Geomorphology 169–170 (2012) 30–44, https://doi.org/10.1016/j.geomorph.2012.01.010.
[5] T.R. Martha, C.J. van Westen, N. Kerle, V. Jetten, K. Vinod Kumar, Landslide hazard and risk assessment using semi-automatically created landslide inventories, Geomorphology 184 (2013) 139–150, https://doi.org/10.1016/j.geomorph.2012.12.001.
[6] B. Peethambaran, D.P. Kanungo, R. Anbalagan, Insights to pre- and post-event stability analysis of rainfall-cum-anthropogenically induced recent Laxmanpuri landslide, Uttarakhand, India, Environ. Earth Sci. 81 (2022), https://doi.org/10.1007/s12665-021-10143-5.
[7] S. Alberti, A. Senogles, K. Kingen, A. Booth, P. Castro, J. DeKoekkoek, K. Glover-Cutter, C. Mohney, M. Olsen, B. Leshchinsky, The Hooskanaden Landslide: historic and recent surge behavior of an active earthflow on the Oregon Coast, Landslides 17 (2020) 2589–2602, https://doi.org/10.1007/s10346-020-01466-8.
[8] B. Peethambaran, V. Nandakumar, K. Sweta, Engineering geological investigation and runout modelling of the disastrous Taliye landslide, Maharashtra, India of 22 July 2021, Nat. Hazards (2023), https://doi.org/10.1007/s11069-023-05985-0.
[9] A. Senogles, M.J. Olsen, B. Leshchinsky, SlideSim: 3D landslide displacement monitoring through a physics-based simulation approach to self-supervised learning, Rem. Sens. 14 (2022), https://doi.org/10.3390/rs14112644.
[10] H. Chen, Z. Zeng, H. Tang, Landslide deformation prediction based on recurrent neural network, Neural Process. Lett. 41 (2015) 169–178.
[11] Y. Yu, M. Shen, H. Sun, Y. Shang, Robust design of siphon drainage method for stabilizing rainfall-induced landslides, Eng. Geol. 249 (2019) 186–197, https://doi.org/10.1016/j.enggeo.2019.01.001.
[12] J. Dou, A.P. Yunus, D. Tien Bui, A. Merghadi, M. Sahana, Z. Zhu, C.W. Chen, K. Khosravi, Y. Yang, B.T. Pham, Assessment of advanced random forest and decision tree algorithms for modeling rainfall-induced landslide susceptibility in the Izu-Oshima Volcanic Island, Japan, Sci. Total Environ. 662 (2019) 332–346, https://doi.org/10.1016/j.scitotenv.2019.01.221.
[13] W. Chen, J. Peng, H. Hong, H. Shahabi, B. Pradhan, J. Liu, A.X. Zhu, X. Pei, Z. Duan, Landslide susceptibility modelling using GIS-based machine learning techniques for Chongren County, Jiangxi Province, China, Sci. Total Environ. 626 (2018) 1121–1135, https://doi.org/10.1016/j.scitotenv.2018.01.124.
[14] J.L. Zêzere, S. Pereira, R. Melo, S.C. Oliveira, R.A.C. Garcia, Mapping landslide susceptibility using data-driven methods, Sci. Total Environ. 589 (2017) 250–267, https://doi.org/10.1016/j.scitotenv.2017.02.188.
[15] H. Hong, B. Pradhan, C. Xu, T.B. Dieu, Spatial prediction of landslide hazard at the Yihuang area (China) using two-class kernel logistic regression, alternating decision tree and support vector machines, Catena 133 (2015) 266–281, https://doi.org/10.1016/j.catena.2015.05.019.
[16] B.T. Pham, D. Tien Bui, I. Prakash, M.B. Dholakia, Hybrid integration of Multilayer Perceptron Neural Networks and machine learning ensembles for landslide susceptibility assessment at Himalayan area (India) using GIS, Catena 149 (2017) 52–63, https://doi.org/10.1016/j.catena.2016.09.007.
[17] O. Rahmati, S. Yousefi, Z. Kalantari, E. Uuemaa, T. Teimurian, S. Keesstra, T.D. Pham, D.T. Bui, Multi-hazard exposure mapping using machine learning techniques: a case study from Iran, Rem. Sens. 11 (2019), https://doi.org/10.3390/rs11161943.
[18] H.R. Pourghasemi, N. Kariminejad, M. Amiri, M. Edalat, M. Zarafshar, T. Blaschke, A. Cerda, Assessing and mapping multi-hazard risk susceptibility using a machine learning technique, Sci. Rep. 10 (2020), https://doi.org/10.1038/s41598-020-60191-3.
[19] T. Yanar, S. Kocaman, C. Gokceoglu, Use of Mamdani fuzzy algorithm for multi-hazard susceptibility assessment in a developing urban settlement (Mamak, Ankara, Turkey), ISPRS Int. J. Geo-Inf. 9 (2020), https://doi.org/10.3390/ijgi9020114.
[20] G. Karakas, S. Kocaman, C. Gokceoglu, A hybrid multi-hazard susceptibility assessment model for a basin in elazig province, türkiye, International Journal of Disaster Risk Science 14 (2023) 326–341, https://doi.org/10.1007/s13753-023-00477-y.
[21] J. Dame, S. Schmidt, J. Müller, M. Nüsser, Urbanisation and socio-ecological challenges in high mountain towns: insights from Leh (Ladakh), India, Landsc. Urban Plann. 189 (2019) 189–199, https://doi.org/10.1016/j.landurbplan.2019.04.017.
[22] P.K. Roy Chowdhury, S. Maithani, Modelling urban growth in the Indo-Gangetic plain using nighttime OLS data and cellular automata, Int. J. Appl. Earth Obs. Geoinf. 33 (2014) 155–165, https://doi.org/10.1016/j.jag.2014.04.009.
[23] D. Turer, H.A. Nefeslioglu, K. Zorlu, C. Gokceoglu, Assessment of geo-environmental problems of the Zonguldak province (NW Turkey), Environ. Geol. 55 (2008) 1001–1014, https://doi.org/10.1007/s00254-007-1049-3.
[24] G.D. Bathrellos, H.D. Skilodimou, A. Kelepertsis, D. Alexakis, I. Chrisanthaki, D. Archonti, Environmental research of groundwater in the urban and suburban areas of Attica region, Greece, Environ. Geol. 56 (2008) 11–18, https://doi.org/10.1007/s00254-007-1135-6.
[25] A. Asgarian, B.J. Amiri, Y. Sakieh, Assessing the effect of green cover spatial patterns on urban land surface temperature using landscape metrics approach, Urban Ecosyst. 18 (2015) 209–222, https://doi.org/10.1007/s11252-014-0387-7.
[26] G.D. Bathrellos, K. Gaki-Papanastassiou, H.D. Skilodimou, D. Papanastassiou, K.G. Chousianitis, Potential suitability for urban planning and industry development using natural hazard maps and geological-geomorphological parameters, Environ. Earth Sci. 66 (2012) 537–548, https://doi.org/10.1007/s12665-011-1263-x.
[27] I.L. Mcharg, Design with Nature, Willey, New York, 1969. www.csiss.org/classics/content/23.
[28] W. Miller, M.G. Collins, F.R. Steiner, E. Cook, An approach for greenway suitability analysis, Landsc. Urban Plann. 42 (1988) 91–105.
[29] A.A. AlFanatseh, Land suitability analysis of urban development in the Aqaba area, Jordan, using a GIS-based analytic hierarchy process, Geojournal 87 (2022) 4143–4159, https://doi.org/10.1007/s10708-021-10488-1.
[30] R.B. Thapa, Y. Murayama, Land evaluation for peri-urban agriculture using analytical hierarchical process and geographic information system techniques: a case study of Hanoi, Land Use Pol. 25 (2008) 225–239, https://doi.org/10.1016/j.landusepol.2007.06.004.
[31] W.A. Ismaeel, J. Satish Kumar, Land suitability analysis of new urban areas using MIF-AHP and bivariate analysis methods in Latakia, Syria, Environ. Dev. Sustain. (2023), https://doi.org/10.1007/s10668-023-03878-7.
[32] A. Bozdağ, F. Yavuz, A.S. Günay, AHP and GIS based land suitability analysis for Cihanbeyli (Turkey) County, Environ. Earth Sci. 75 (2016), https://doi.org/10.1007/s12665-016-5558-9.
[33] S. Baja, D.M. Chapman, D. Dragovich, Spatial based compromise programming for multiple criteria decision making in land use planning, Environ. Model. Assess. 12 (2007) 171–184, https://doi.org/10.1007/s10666-006-9059-1.
[34] F.C. Dai, C.F. Lee, X.H. Zhang, GIS-based geo-environmental evaluation for urban land-use planning: a case study, Eng. Geol. 61 (2001) 257–271. www.elsevier.com/locate/enggeo.
[35] S. Park, S. Jeon, S. Kim, C. Choi, Prediction and comparison of urban growth by land suitability index mapping using GIS and RS in South Korea, Landsc. Urban Plann. 99 (2011) 104–114, https://doi.org/10.1016/j.landurbplan.2010.09.001.
[36] K. Kushwaha, M.M. Singh, S.K. Singh, A. Patel, Urban growth modeling using earth observation datasets, Cellular Automata-Markov chain model and urban metrics to measure urban footprints, Remote Sens. Appl. 22 (2021), 100479, https://doi.org/10.1016/j.rsase.2021.100479.
[37] Y. Cao, X. Zhang, Y. Fu, Z. Lu, X. Shen, Urban spatial growth modeling using logistic regression and cellular automata: a case study of Hangzhou, Ecol Indic 113 (2020), 106200, https://doi.org/10.1016/j.ecolind.2020.106200.
[38] S. Al-Kheder, J. Wang, J. Shan, Fuzzy inference guided cellular automata urban-growth modelling using multi-temporal satellite images, Int. J. Geogr. Inf. Sci. 22 (2008) 1271–1293, https://doi.org/10.1080/13658810701617292.
[39] J.M.C. Pereira, L. Duckstein, A multiple criteria decision-making approach to gis-based land suitability evaluation, Int. J. Geogr. Inf. Syst. 7 (1993) 407–424, https://doi.org/10.1080/02693799308901971.
[40] R. Liu, K. Zhang, Z. Zhang, A.G.L. Borthwick, Land-use suitability analysis for urban development in Beijing, J. Environ. Manag. 145 (2014) 170–179, https://doi.org/10.1016/j.jenvman.2014.06.020.
[41] S. Bamrungkhul, T. Tanaka, The assessment of land suitability for urban development in the anticipated rapid urbanization area from the Belt and Road Initiative: a case study of Nong Khai City, Thailand, Sustain. Cities Soc. 83 (2022), https://doi.org/10.1016/j.scs.2022.103988.
[42] G.D. Bathrellos, H.D. Skilodimou, K. Chousianitis, A.M. Youssef, B. Pradhan, Suitability estimation for urban development using multi-hazard assessment map, Sci. Total Environ. 575 (2017) 119–134, https://doi.org/10.1016/j.scitotenv.2016.10.025.

[43] E.H. Mamdani, S. Assilian, An experiment in linguistic synthesis with a fuzzy logic controller, Int. J. Man Mach. Stud. 7 (1975) 1–13.
[44] J. Marull, J. Pino, J.M. Mallarach, M.J. Cordobilla, A land suitability index for strategic environmental assessment in metropolitan areas, Landsc. Urban Plann. 81 (2007) 200–212, https://doi.org/10.1016/j.landurbplan.2006.11.005.
[45] B. Peethambaran, R. Anbalagan, K.V. Shihabudheen, Landslide susceptibility mapping in and around Mussoorie Township using fuzzy set procedure, MamLand and improved fuzzy expert system-A comparative study, Nat. Hazards 96 (2019) 121–147, https://doi.org/10.1007/s11069-018-3532-4.
[46] V. Kreinovich, O. Kosheleva, S.N. Shahbazova, Why triangular and trapezoid membership functions: a simple explanation, in: Studies in Fuzziness and Soft Computing, 2020, pp. 25–31. http://www.springer.com/series/2941.
[47] W. Pedrycz, Why triangular membership functions? Fuzzy Set Syst. 64 (1994) 21–30, https://doi.org/10.1016/0165-0114(94)90003-5.
[48] D. Ruan, E.E. Kerre, Fuzzy implication operators and generalized fuzzy method of cases, Fuzzy Set Syst. 54 (1993) 23–37, https://doi.org/10.1016/0165-0114(93)90357-N.
[49] K.S. Valdiya, Geology of Kumaun Lesser Himalaya, Wadia Institute of Himalayan Geology, Dehradun, 1980.
[50] G.F. Jenks, The Data Model Concept in Statistical Mapping, International Yearbook of Cartography, 1967.
[51] L.L.C. Google, Google Earth, 2003, Version 9.4.0. https://www.google.com/earth/.
[52] B. Peethambaran, R. Anbalagan, D.P. Kanungo, A. Goswami, K.V. Shihabudheen, A comparative evaluation of supervised machine learning algorithms for township level landslide susceptibility zonation in parts of Indian Himalayas, Catena 195 (2020), 104751, https://doi.org/10.1016/j.catena.2020.104751.
[53] K.V. Shihabudheen, G.N. Pillai, Regularized extreme learning adaptive neuro-fuzzy algorithm for regression and classification, Knowl. Base Syst. 127 (2017) 100–113.
[54] K.V. Shihabudheen, B. Peethambaran, Landslide displacement prediction technique using improved neuro-fuzzy system, Arabian J. Geosci. 10 (2017) 502, https://doi.org/10.1007/s12517-017-3278-4.
[55] K.V. Shihabudheen, G.N. Pillai, B. Peethambaran, Prediction of landslide displacement with controlling factors using extreme learning adaptive neuro-fuzzy inference system (ELANFIS), Applied Soft Computing Journal 61 (2017) 892–904, https://doi.org/10.1016/j.asoc.2017.09.001.
[56] B. Peethambaran, R. Anbalagan, K.V. Shihabudheen, A. Goswami, Robustness evaluation of fuzzy expert system and extreme learning machine for geographic information system-based landslide susceptibility zonation: a case study from Indian Himalaya, Environ. Earth Sci. 78 (2019), https://doi.org/10.1007/s12665-019-8225-0.